ORIGINAL ARTICLE

Cell
Proliferation WILEY

Conditioned medium derived from 3D tooth germs: A novel cocktail for stem cell priming and early in vivo pulp regeneration

Tengfei Zhou[1] | Mingdeng Rong[1] | Zijie Wang[2] | Hongxing Chu[1] | Chuying Chen[2] | Jiayi Zhang[2] | Zhihui Tian[2,3]

[1]Department of Periodontology and Oral Implantology, Stomatological Hospital, Southern Medical University, Guangzhou, China

[2]Department of Stomatology, Nanfang Hospital, Southern Medical University, Guangzhou, China

[3]School of Stomatology, Southern Medical University, Guangzhou, China

Correspondence
Zhihui Tian, Department of Stomatology, Nanfang Hospital, Southern Medical University, 510515 Guangzhou, China.
Email: Tianzh@i.smu.edu.cn

Abstract

Objectives: Conditioned medium (CM) from 2D cell culture can mitigate the weakened regenerative capacity of the implanted stem cells. However, the capacity of 3D CM to prime dental pulp stem cells (DPSCs) for pulp regeneration and its protein profile are still elusive. We aim to investigate the protein profile of CM derived from 3D tooth germs, and to unveil its potential for DPSCs-based pulp regeneration.

Materials and Methods: We prepared CM of 3D ex vivo cultured tooth germ organs (3D TGO-CM) and CM of 2D cultured tooth germ cells (2D TGC-CM) and applied them to prime DPSCs. Influences on cell behaviours and protein profiles of CMs were compared. In vivo pulp regeneration of CMs-primed DPSCs was explored using a tooth root fragment model on nude mice.

Results: TGO-CM enhanced DPSCs proliferation, migration, in vitro mineralization, odontogenic differentiation, and angiogenesis performances. The TGO-CM group generated superior pulp structures, more odontogenic cells attachment, and enhanced vasculature at 4 weeks post-surgery, compared with the TGC-CM group. Secretome analysis revealed that TGO-CM contained more odontogenic and angiogenic growth factors and fewer pro-inflammatory cytokines. Mechanisms leading to the differential CM profiles may be attributed to the cytokine–cytokine receptor interaction and PI3K-Akt signalling pathway.

Conclusions: The unique secretome profile of 3D TGO-CM made it a successful priming cocktail to enhance DPSCs-based early pulp regeneration.

1 | INTRODUCTION

Dental pulp stem cells (DPSCs) offer practical advantages such as accessibility, self-renewal, multipotency, and immunomodulation,[1] making DPSC-based tissue engineering increasingly attractive in pulp–dentin complex regeneration from bench to bedside.[2,3] However, direct mesenchymal stem cells (MSC) administration presents limitations such as transplanted cells' low survival, trans-differentiation rates,[4]

Zhou and Rong these two authors contributed equally to this study.

and compromised regenerative functions.[5] Donor systemic diseases and senescence can also impair the MSC reparative capacity,[6,7] with unsatisfactory clinical trial outcomes.[8–10]

In vitro MSC priming is a promising technique in circumventing these shortcomings by modulating the secretome,[11] with hypoxia, cytokines, and 3D cell culture proposed as in vitro priming stimuli.[12–15] Conditioned medium (CM), the supernatant collected from the cell culture medium, contains the MSC secretome, which includes extracellular matrix components, growth factors, and cytokines.[16] Already being broadly used,[17] CM priming can promote tissue regeneration, angiogenesis, immunomodulation, and anti-fibrosis.[18] DPSC-derived CMs can recapitulate parent MSC functions, suggesting potential in dental and extra-oral tissue engineering applications.[19]

Most current CM types are harvested from 2D cell culture,[17] including tooth germ cell-derived CM (TGC-CM).[20–22] Nevertheless, living systems like tooth germ organs (TGOs) exist in well-organized 3D arrangements with intricate cellular and extracellular interactions; these in vivo bioprocesses can barely be replicated by 2D monolayer cell cultures. In contrast, 3D cell cultures create more accurate physiological simulations of in vivo microenvironments, with gene and protein expression closely resembling those within original living systems.[23,24] As pulpogenesis is orchestrated by bio-factors secreted by mesenchymal and epithelial cells within the tooth germ during embryonic development,[25] we reasonably deduced that tooth germ-derived CM would contain a semblable tooth germ protein profile which could orchestrate pulp repair under physiological and pathological scenarios.

While the literature on 2D CM-based DPSC-priming abounds, few studies have addressed 3D CM-based DPSC-priming for pulp regeneration.[19] Only a few studies have analysed the protein profile of 2D CM derived from DPSCs.[26,27] It remains unclear whether and how CM of 3D tooth germ organ (TGO-CM) will impact on pulp regeneration.

Due to its secretome biomimicry, we hypothesized that 3D TGO-CM would triumph over its 2D counterpart in promoting early pulp regeneration. We compared the effects of 3D TGO-CM and 2D TGC-CM on in vitro DPSC proliferation, migration, differentiation, and mineralization, and on in vivo pulp regeneration after 4 weeks. Additionally, we analysed the compositional differences between the two CMs and explored the resulting biomechanisms. To the best of our knowledge, this study is the first to report the protein profile of 3D cultured tooth germs and the first to unveil its potential in priming DPSCs for early in vivo pulp regeneration. Our results may shed light on stem cell priming for pulp regeneration using a trace-back-to-organ approach.

2 | MATERIALS AND METHODS

2.1 | Cell culture and CM preparation

2.1.1 | Isolation and cell culture of human DPSCs and mouse TGCs

Newly extracted healthy human third molars and premolars were collected from healthy anonymous patients (18–25 years), with approval from the Institutional Review Board of the Stomatological Hospital, Southern Medical University (201806), and informed consents from all patients. Teeth were stored in culture medium and immediately delivered to the laboratory for further processing. Mandibular first molar tooth germs from newborn CD-1 mice were surgically dissected following a previously reported protocol.[28] All animal experiments conformed to related ethical principles.

Human DPSCs and mouse TGCs were isolated as previously reported[28] and cultured in L-DMEM supplemented with 15% foetal bovine serum (FBS), 100 U/ml penicillin-G, and 100 mg/ml streptomycin, under 5% CO_2 at 37°C. The culture medium was refreshed every 2–3 days. Cells were passaged when they reached 80% confluency and expanded for all experiments at passages 3–5.

2.1.2 | Immunofluorescent staining of mouse TGCs

Immunofluorescent staining was performed as per the manufacturer's instructions, using anti-CK14 and anti-vimentin antibodies (Abcam, Cambridge, UK) and treated with related secondary antibodies. Samples were blocked using Vectashield mounting medium containing DAPI. Images were captured using a confocal immunofluorescence microscope.[29]

2.1.3 | Preparation of 2D TGC-CM

At 80% confluency, the TGC medium was replaced with FBS-free L-DMEM. After 16 h, the resulting medium was collected, filtered, and centrifuged at 1,000 rpm for 5 min at 4°C. The supernatant was harvested as 2D TGC-CM, stored at −80°C, and used without concentration.

2.1.4 | Preparation of 3D TGO-CM

Fifteen TGOs of newborn mice were 3D ex vivo cultured in 1-ml FBS-free L-DMEM under 5% CO2 at 37°C. The medium was refreshed at the same time intervals as the TGC-CM culture. At 8, 16, and 24 h, the resulting medium was collected, filtered, and centrifuged at 1,000 rpm for 5 min at 4°C. The supernatant was harvested as 3D TGO-CM, stored at −80°C, and used without concentration.

2.1.5 | Hoechst/TUNEL staining of TGOs

Paraffin-embedded TGO samples were sectioned into 5-μm slices at timed intervals, stained using a TUNEL Apoptosis Detection Kit (Vazyme Biotech, Nanjing, China) following the manufacturer's protocol, and subjected to Hoechst 33342 staining (Solarbio, Beijing, China). Unstained sections were stained with hematoxylin and eosin (H&E; Solarbio). The images were visualized using a fluorescent microscope.

2.1.6 | Cell viability assay of TGOs

A Live Dead Cell Viability Assay Kit (Sigma-Aldrich, St. Louis, MO) was used according to the manufacturer's protocol. TGOs at 8, 16, and 24 h were stained with calcein AMAM (green, live cells) and propidium iodide (red, dead cells). Images were captured using a fluorescence microscope.

2.2 | In vitro DPSCs behaviours

2.2.1 | DPSCs priming with CMs

Conditioned mediums harvested at 16 h were used to prime DPSCs. L-DMEM supplemented with 15% FBS was used in the control medium group in all assays. In the TGC-CM and TGO-CM group, L-DMEM was supplemented with 15% FBS for cell proliferation and migration assays or supplemented with 15% FBS containing related osteoinductive ingredients (1% penicillin/streptomycin, 50 μg/ml ascorbic acid, 10 nmol/L dexamethasones, and 5 mmol/L β-glycerophosphate) for in vitro odontogenic/osteogenic differentiation assays. All groups were incubated under 5% CO_2 at 37°C.

2.2.2 | Cell proliferation assay

Dental pulp stem cells were seeded at 10,000/well in 96-well plates and cultured for 5 days. CCK-8 assay was conducted as per the manufacturer's protocol on days 1–5, and cell viability was measured via UV spectrophotometry using absorbance at 450 nm.

2.2.3 | Transwell cell migration assay

Assays were conducted, according to the manufacturer's instructions. In brief, DPSCs cultured in TGC-CM, TGO-CM, and control medium were digested and resuspended, respectively. 2×10^5 DPSCs from each of three groups were seeded into the upper chambers containing FBS-free L-DMEM in all groups. The lower chambers contained 15% FBS-supplemented L-DMEM in all groups. After a 24-h incubation, migrated cells were stained with 0.1% crystal violet, and quantitative analysis was performed by cell counting using ImageJ software (National Institute of Health).

2.3 | In vitro odontogenic differentiation

2.3.1 | Alizarin Red S staining

Osteogenic inductive ingredients were added into all medium groups when DPSCs reached 80% confluency. After 3 weeks, cells were fixed with 4% paraformaldehyde, washed, and stained with Alizarin Red S (Sigma-Aldrich) for 20 min. The formation of mineralized nodules was observed under a microscope. Quantitative data were obtained by solubilizing the samples with 10% cetylpyridinium chloride solution (CPC, Sigma-Aldrich) and measuring their optical density at 490 nm.

2.3.2 | Quantitative real-time polymerase chain reaction (RT-qPCR)

Total cellular RNA was extracted using TRIzol reagent (Invitrogen, Waltham, MA), and PCR was conducted using SYBR Premix Ex Taq (Takara, Shiga, Japan) and iCycler (Bio-Rad, Feldkirchen, Germany), according to the manufacturers's protocol. Relative transcription levels of human dentin matrix protein 1 (DMP 1), dentin sialophosphoprotein (DSPP), bone sialoprotein (BSP), and osterix (OSX) were analysed using glyceraldehyde-3-phosphate dehydrogenase (GAPDH) as a normalized reference. Forward and reverse primers used are listed in Table S1.[30,31]

2.3.3 | Western Blot assay

Seven days after osteoinduction, Western blotting was conducted as described in our previous study,[28] using primary antibodies against DMP 1 (ab103203, Abcam), DSPP (sc-73632, Santa Cruz Biotechnology, Dallas, TX), BSP (ab52128, Abcam), OSX (ab94744, Abcam), and VEGF (sc-57496, Santa Cruz Biotechnology), with GAPDH as an internal control. Membranes were visualized using a chemiluminescent reagent (Sigma-Aldrich) under a Western blotting imaging system (Bio-Rad, Hercules, CA), and protein expression was quantified using ImageJ software.

2.4 | Animal experiment on a semi-orthotopic tooth root fragment model

2.4.1 | Preparation of root fragments of human teeth

Mature single-root premolars without previous root canal treatment were collected from adult patients. Tooth root fragments were prepared as previously reported.[32] Briefly, 5-mm fragments were sectioned with pulp tissue, pre-dentin, and partial dentin removed. Canals were enlarged to 3 mm in diameter, treated with 5% EDTA for 5 min, and subjected to ultrasonic treatment for 10 min. The larger end was then sealed with mineral trioxide aggregate. Fragments were stored in PBS containing 50 mg/ml streptomycin and 50 U/ml penicillin at 4°C and disinfected by UV sterilization. The fluid hydrogel containing 4×10^5 DPSCs from each group was injected into the canal cavity of root fragments. The hydrogel-DPSCs compounds jelled quickly to prevent leakage.

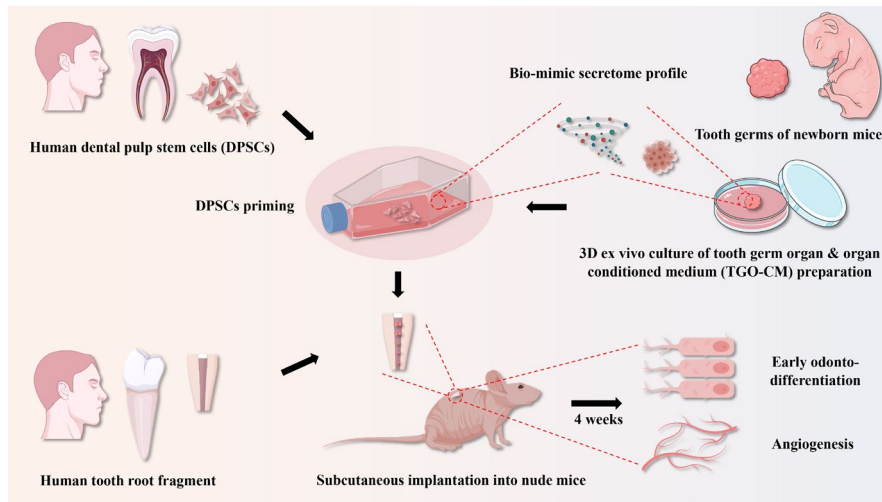**FIGURE 1** Illustration of 3D TGO-CM primed DPSCs for early dental pulp regeneration

2.4.2 | Subcutaneous implantation into nude mice

Animal experiments were approved by the Institutional Review Board of the Stomatological Hospital, Southern Medical University (201806) and conformed to ethical principles. Surgical procedures were performed as previously reported.[32] Briefly, surgery was performed on 6-week-old immunocompromised nude mice ($n = 12$) under general anaesthesia. A single hydrogel-DPSCs filled fragment was transplanted subcutaneously into the dorsal side of each mouse. All mice were euthanized at 4 weeks post-surgery, and all fragments were collected.

2.4.3 | Histological assay

As per our previous protocol, fragments were fixed in 4% paraformaldehyde overnight, decalcified for 3 months using 10% EDTA, embedded in paraffin, sectioned into 5-μm slices, and subjected to H&E and Masson's trichrome staining (Solarbio, Beijing, China). Histomorphology was observed using Scanscope CS and Image Scope software (Aperio, Sausalito, CA). Quantitative analysis was conducted using ImageJ software to measure the percentage of regenerated pulp tissue area inside the root canal, the percentage of pulpal blood vessel area, and the number of cells attached to the dentin wall.

2.4.4 | Odontogenic immunohistochemical staining

Immunohistochemistry analysis was conducted using an HRP-DAB Cell & Tissue Staining Kit (R&D Systems, Minneapolis, MN). Briefly, samples were deparaffinized, blocked, and incubated with anti-DMP1 (Abcam) overnight at 4°C, followed by incubation with horseradish peroxidase-conjugated secondary antibodies for 30 min after sample washing. Histometric observations were performed as the methods in the histological assay.

2.5 | Proteome cytokine array of CMs

Secretome analysis was conducted using a Proteome Profiler Mouse XL Cytokine Array kit ARY028 (R&D Systems) following the manufacturer's protocol. TGO-CM and TGC-CM at 16 h were screened for a total of 111 biofactors. Gene ontology enrichment analysis (GOEA) and Kyoto Encyclopedia of Genes and Genomes (KEGG) enrichment analysis were conducted. Data were visualized using an InnoScan 300 Microarray Scanner and analysed using GenePix Pro software and RayBiotech Q-Analyzer software (RayBiotech, Inc., Shanghai, China).

2.6 | Statistical analysis

Data analysis and graphical preparation were conducted using GraphPad Prism 8.3. Data are described as mean ±standard deviation and replicated for three independent experiments. One-way ANOVA with Tukey's multiple comparison test was performed to detect statistical differences. Statistical significance was set at $p < 0.05$.

3 | RESULTS

The study design is depicted in Figure 1.

FIGURE 2 Tooth germs consisted of mesenchymal and epithelial cells. (A, D, G) tooth germ cells (TGCs) at days 1, 3, 5. TGCs were a mixture of different cell types and proliferated at a fast tempo. (B, E, H) Epithelial cells in TGCs at days 1, 3, 5 were cobblestone-like. (C, F, I) Mesenchymal cells at day 1, 3, 5 were spindle-like. (J–M) cobblestone-like and spindle-like cells were positively stained by epithelial marker CK14 and mesenchymal marker vimentin, respectively
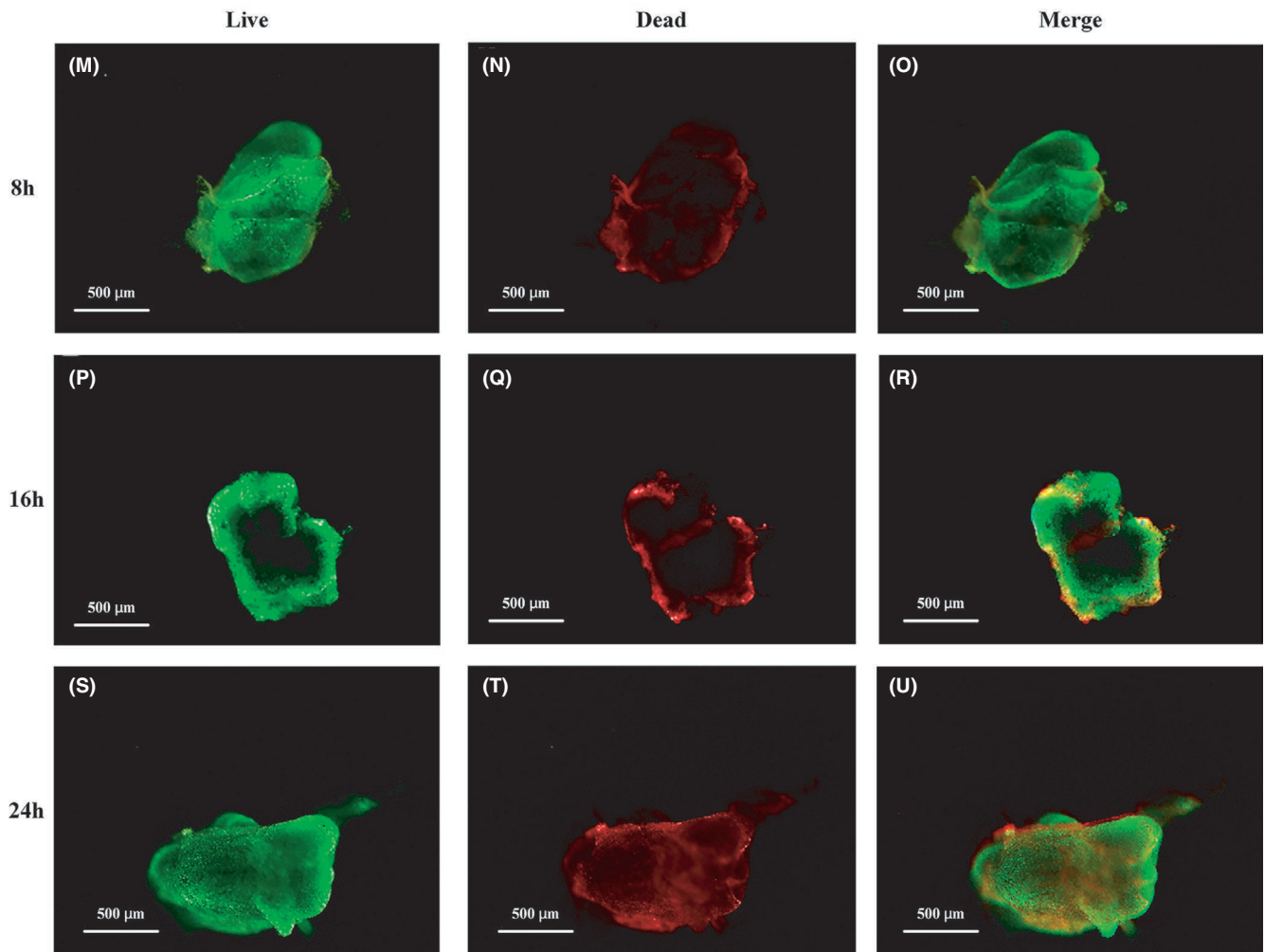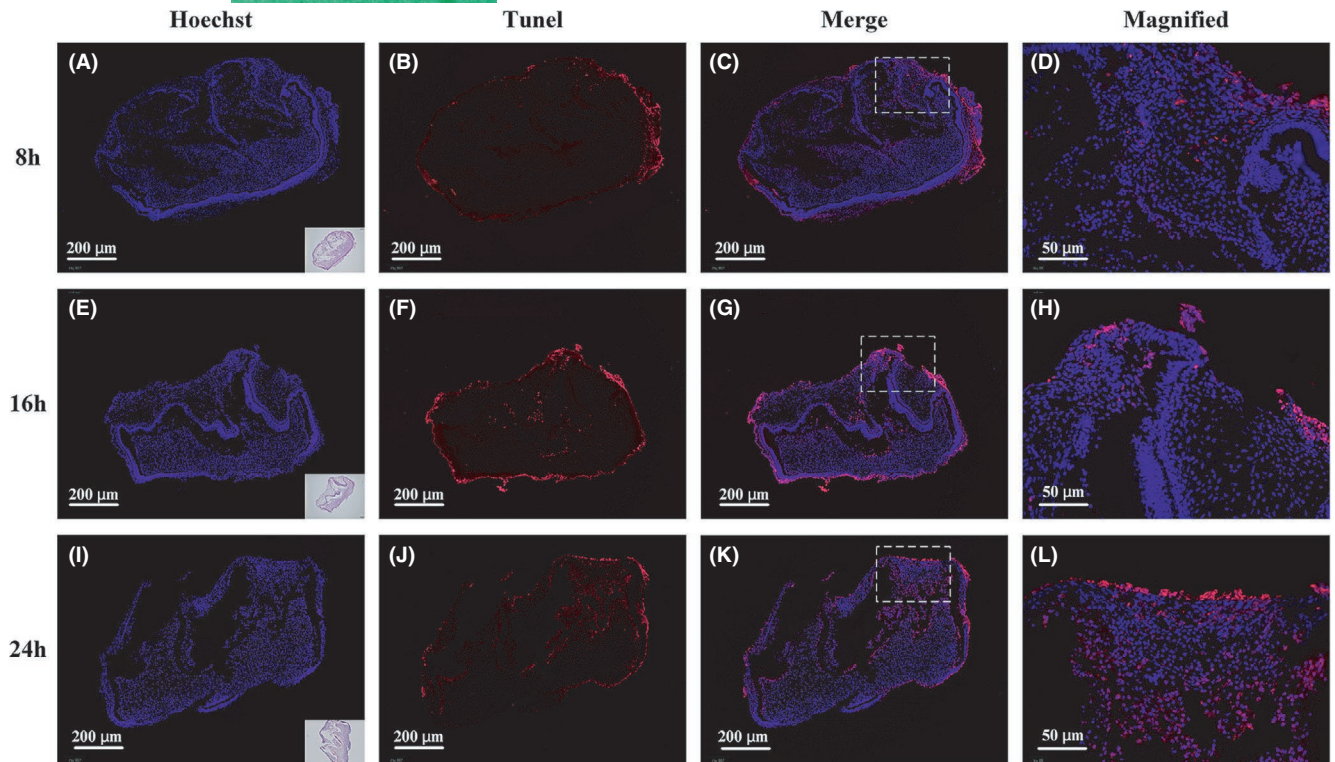
WILEY—Cell Proliferation

ZHOU ET AL.
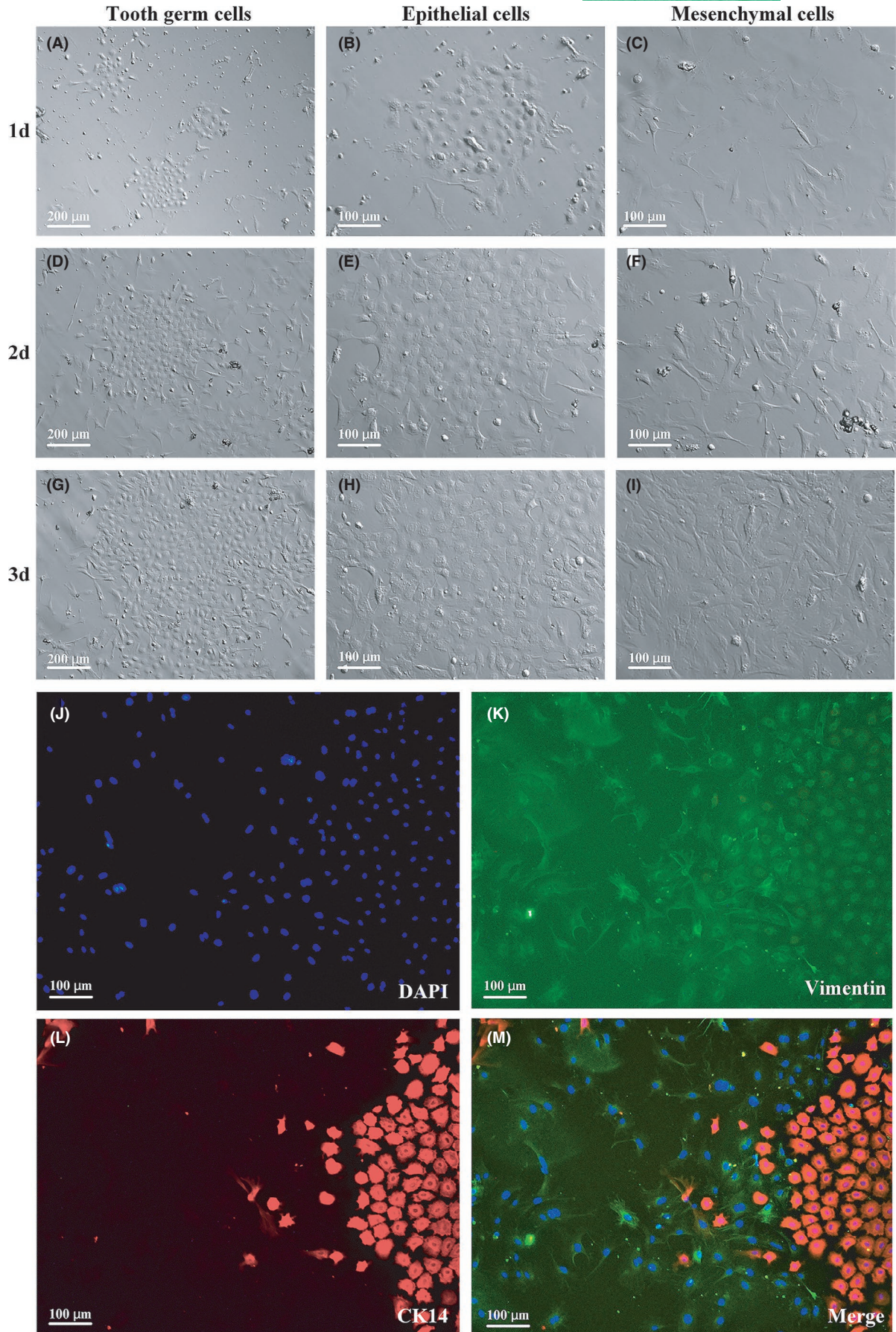
FIGURE 3 Viability of tooth germs under 3D ex vivo culture. (A–D) Cell apoptosis inside germs was undetectable at 8 h. (E–H) Slight cell apoptosis emerged at 16 h. (I–L) Grave cell apoptosis inside germs appeared at 24 h. (M–O) Cell necrosis inside germs was undetectable at 8 h. (P–R) Slight cell necrosis emerged at the centre of germs at 16 h. (S–U) Grave cell necrosis appeared at the centre of germs at 24 h. White dotted squares: (D, H, L) represented the magnified regions of (C, G, K), respectively
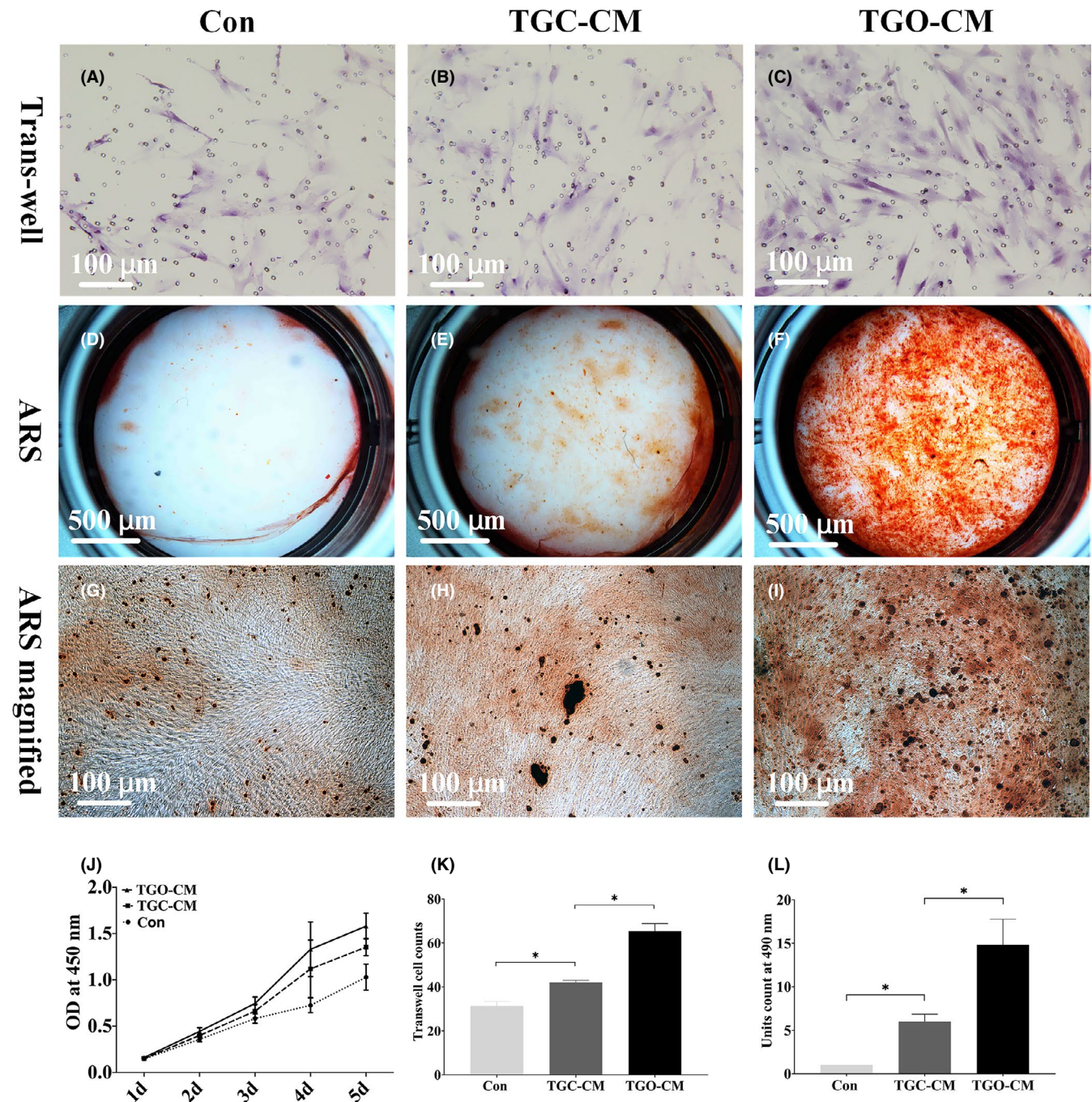

FIGURE 4 CM of 3D ex vivo cultured tooth germ organs enhanced in vitro DPSCs proliferation, migration, and in vitro mineralization. (A–C) Migrated DPSCs at 24 h primed by control medium, TGC-CM, and TGO-CM, respectively. (D–I) Alizarin Red S staining of DPSCs primed by control medium, TGC-CM, and TGO-CM for 3 weeks, respectively. (J–L) Quantitative data of DPSCs proliferation, migration, and ARS mineralized units, respectively. * indicated $p < .05$

3.1 | Cell types within tooth germs

Tooth germ cells from digested tooth germ explants (Figure 2) reached 90% confluence by day 3. Under a telescope (Figure 2A,D,G), TGCs appear to be a mixture of epithelial-like cells, with an oval cobblestone appearance (Figure 2B,E,H), and mesenchymal-like cells, presenting in polygonal, triangular, and spindle-like forms (Figure 2C,F,I). Immunofluorescent staining (Figure 2J–M) showed that the epithelial marker CK14 stained the cobblestone-like cells red, while the mesenchymal marker vimentin stained the spindle-like cells green.
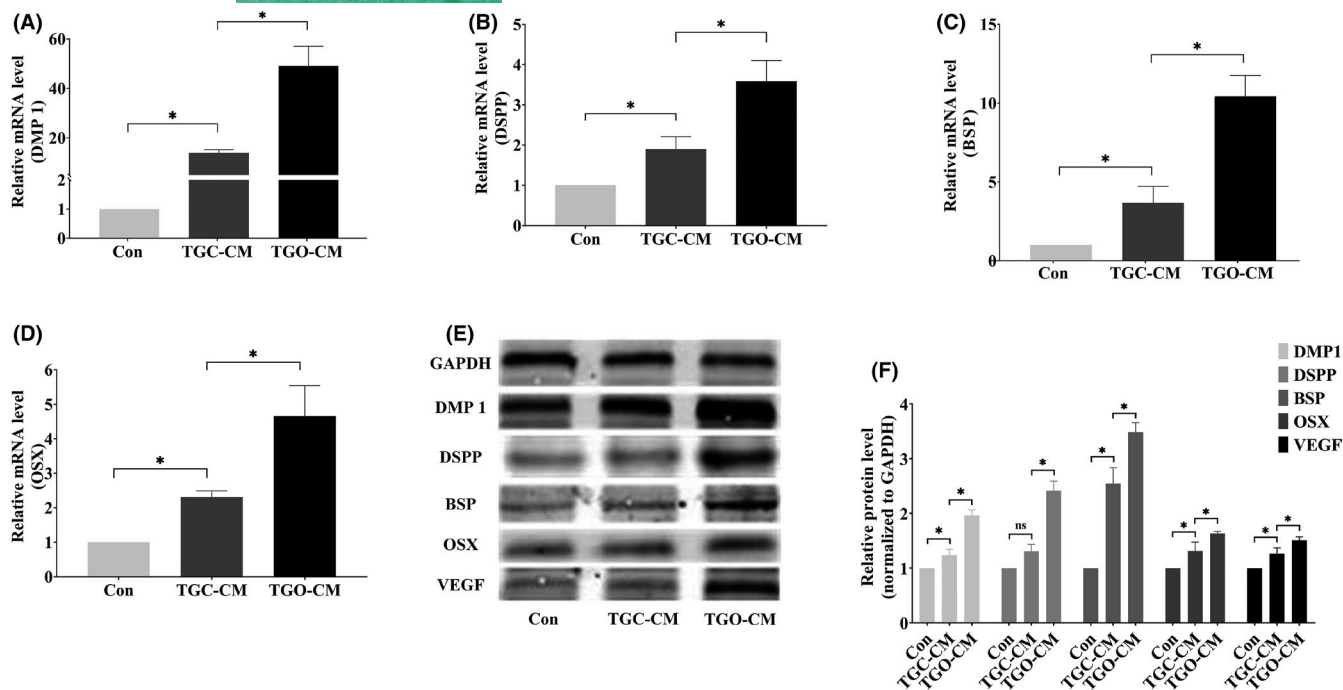
FIGURE 5 Odontogenic and angiogenic differentiation. (A–D) Expression of DMP 1, DSPP, BSP, OSX genes was elevated at mRNA level in the TGO-CM group. (E–F) Expression of DMP 1, DSPP, BSP, OSX, VEGF was elevated at the protein level in the TGO-CM group. * indicated $p < .05$, and "ns" suggested non-significant

3.2 | Viability of tooth germs under 3D ex vivo culture

The Hoechst/TUNEL staining indicated that cell apoptosis within tooth germ was undetectable at 8 h, emerging at 16 h, and peaking at 24 h (Figure 3A–L). Similarly, at 8 h, the red damaged parts were barely seen inside the germ except for on the nonspecific margins; at 16 h, slight tissue necrosis (red) was observed at the centre, with the vast outer layer stained in green, indicating living tissue; at 24 h, severe tissue damage was indicated by an enlarged red core (Figure 3M–U).

3.3 | TGO-CM enhanced in vitro DPSCs behaviour

Transwell migration assay revealed that the TGO-CM group presented the most migrated cells (Figure 4A–C). Similarly, Alizarin Red S staining revealed a higher level of mineralized deposition in the TGO-CM group (Figure 4D–I).

Quantitatively, DPSCs primed by TGO-CM proliferated more quickly and had increased by 0.56 ± 0.28 and 0.22 ± 0.14 folds, respectively, compared to the control group and TGC-CM group at day 5 ($p < 0.05$, Figure 4J). The number of migrated DPSCs in the TGO-CM group was 1.09 ± 0.19 and 0.55 ± 0.12 folds greater than those of the control group and TGC-CM group, respectively ($p < 0.0001$, Figure 4K). The ARS unit count in the TGO-CM group was significantly larger, by 13.81 ± 2.96 and 8.81 ± 2.48 folds, compared to those of the control group and TGC-CM group, respectively ($p < 0.01$, Figure 4L).

3.4 | CM gene expression and protein levels

Odontogenesis-related gene expression in the TGO-CM group was notably elevated at the mRNA transcription level (Figure 5A–D). The relative gene expressions of the TGO-CM group compared with the control and TGC-CM groups were as follows, each, respectively: DMP 1, 49.10 ± 7.97 and 3.48 ± 0.27 folds greater; DSPP, 3.59 ± 0.51 and 1.89 ± 0.07 folds greater; BSP, 10.43 ± 1.32 and 3.04 ± 1.06 folds greater; and OSX, 4.66 ± 0.89 and 2.02 ± 0.40 folds greater ($p < 0.01$).

Odontogenic and angiogenic protein levels were elevated in the TGO-CM group (Figure 5E). The relative protein levels of the TGO-CM group compared with the control and TGC-CM groups were as follows, each, respectively: DMP 1, 1.96 ± 0.10 and 1.59 ± 0.11 folds greater; DSPP, 2.42 ± 0.17 and 1.86 ± 0.20 folds greater; BSP, 3.49 ± 0.17 and 1.38 ± 0.14 folds greater; OSX, 1.64 ± 0.03 and 1.26 ± 0.13 folds greater; and VEGF, 1.51 ± 0.06 and 1.20 ± 0.11 folds greater ($p < 0.05$, Figure 5F).

3.5 | In vivo dental pulp regeneration

Within the 4 weeks, all surgical sites healed without observable inflammation, infection, or graft exposure. The grafted hydrogel was fully degraded in all groups (Figure 6). Root canals in the control group were filled with fibre-rich tissue containing a trivial number of cells. The resulting mass of poorly organized, deformed, hypo-vascular connective tissue bore no similarities to pulp tissue (Figure 6A,D,G,J). The TGC-CM group demonstrated increased cells
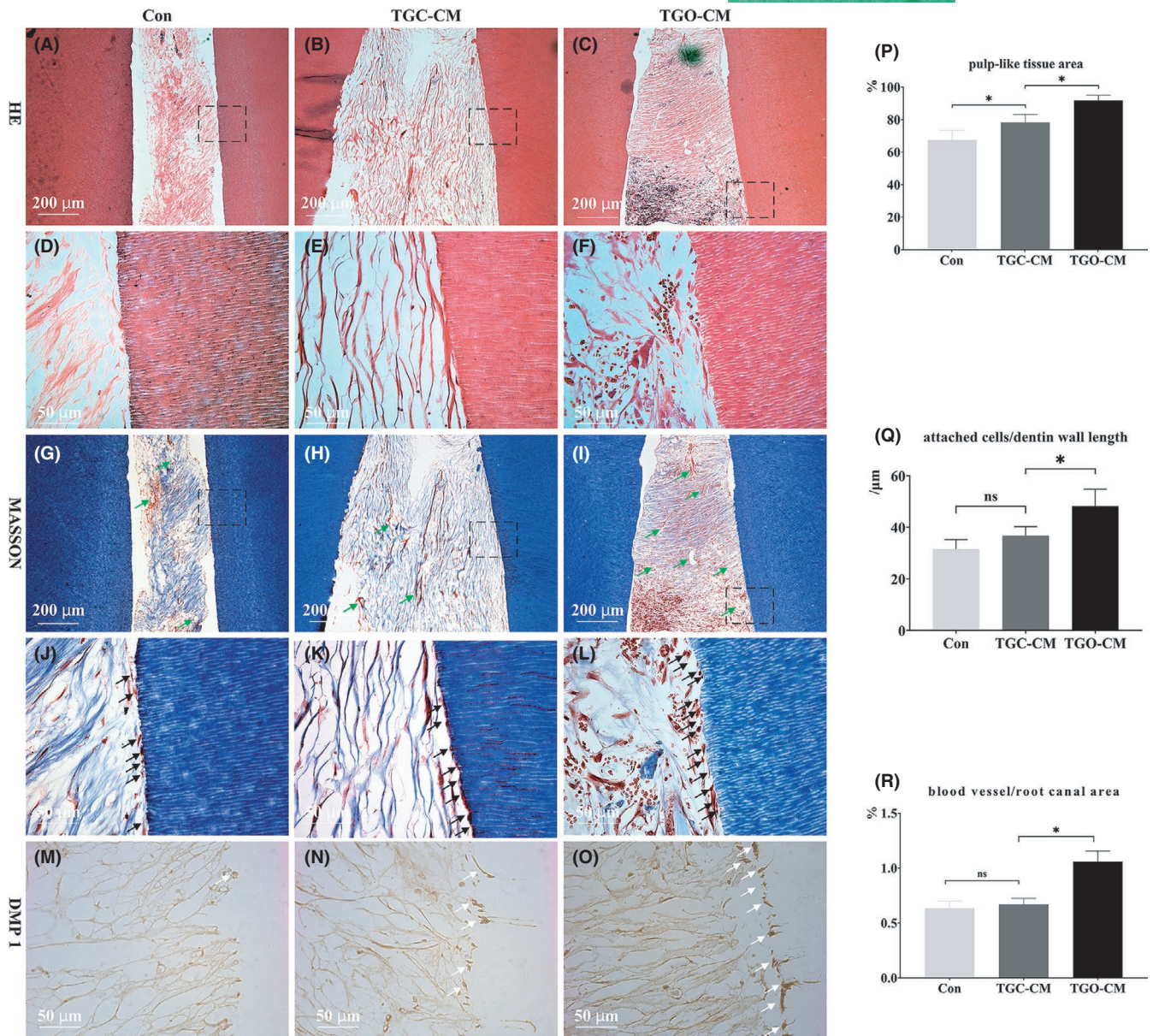
FIGURE 6 CM of 3D ex vivo cultured tooth germ organs promoted in vivo pulp regeneration. (A, D, G, J) and (B, E, H, K) Poorly organized and hypo-vascular connective tissue healed in the control group and TGC-CM group, respectively. (C, F, I, L) Well-organized and vascularized pulp tissue regenerated in the TGO-CM group. (M–O) The attached cell layer in the TGO-CM group was deeply stained with DMP 1, indicating the odontogenic odontoblast-like cells. (P–R) 3D TGO-CM increased the area of regenerated pulp-like tissue and the number of attached cells and blood vessels. Black dotted squares: (D, E, F) and (J, K, L) represented the magnified regions in (A, B, C) and (G, H, I), respectively. Green arrows: blood vessels. * indicated $p < .05$, and "ns" suggested non-significant

and capillary vessels but without organized pulp tissue structure (Figure 6B,E,H,K). As depicted in Fig. C and I, canals of the TGO-CM group were almost filled with compacted connective tissue. The pulp-like tissue was well structured with ECM, collagen, abundant cells, and a robust blood vessel network (green arrows, Figure 6C,F,I,L). Higher Masson magnifications (Figure 6J–L) revealed an uneven cell layer situated at the dentin–pulp interface, attached to the dentin wall, in both the TGM-CM and TGO-CM groups. However, cells in the former displayed a flat appearance, while those of the latter appeared more columnar. Immunohistochemical staining of DMP 1, an odontogenic marker, revealed deeper staining in the attached cell layer in the TGO-CM group, identifying odontogenic odontoblast-like cells (white arrows, Figure 6M–O). However, no visible mineralized dentin-like tissue formation or detectable odontoblast polarity was detected in all groups.

Quantitatively, the characteristics of the TGO-CM group in comparison with the control and TGC-CM groups were as follows, each, respectively: pulp-like tissue filling rate, 0.92 ± 0.03 in the TGO-CM, and 0.37 ± 0.11 and 0.18 ± 0.12 folds greater ($p < 0.01$); number of attached cells, 0.54 ± 0.21 and 0.31 ± 0.13 folds greater ($p < 0.05$); blood vessel area rate, 0.69 ± 0.30 and 0.60 ± 0.27 folds greater ($p < 0.01$) (Figure 6P–R).
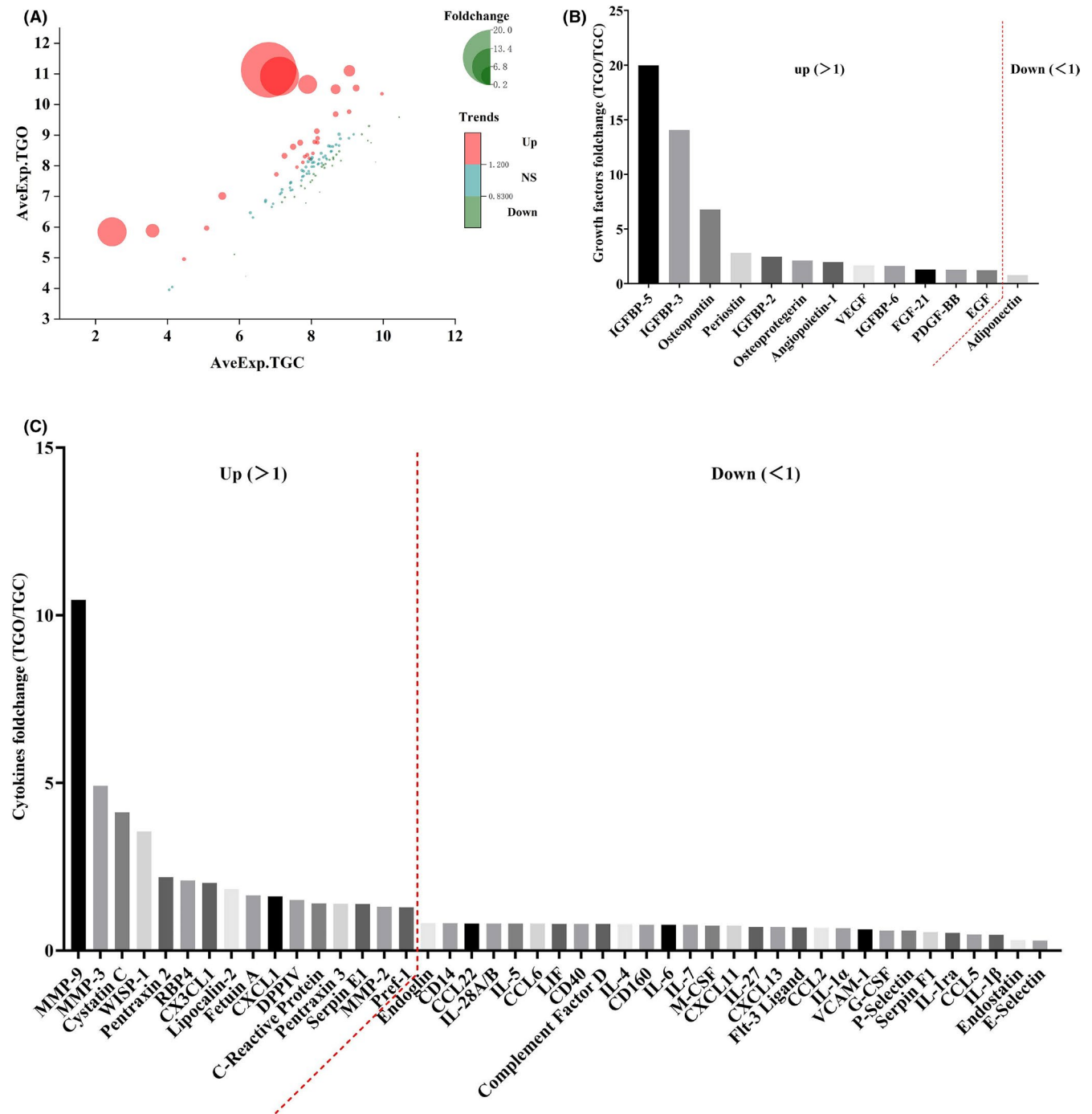
FIGURE 7 Protein profile differences between TGO-CM and TGC-CM. (A) Fifty-eight types of differential proteins were detected with statistical significance. (B) TGO-CM contained higher levels of growth factor types. (C) TGO-CM contained fewer pro-inflammatory cytokines

3.6 | Protein profile assay of CMs

Of the 111 proteins screened, 58 were detected with statistical significance in both CM types (Figure 7A). TGO-CM contained higher levels of insulin-like growth factor-binding protein 3 and 5 (IGFBP 3 and 5, 14.05- and 19.99 folds, respectively), osteopontin (6.79 folds), periostin (2.82 folds), osteoprotegerin (2.11 folds), angiopoietin-1 (1.97 folds), VEGF (1.66 folds), fibroblast growth factor (FGF, 1.28 folds), platelet-derived growth factor (PDGF, 1.27 folds), and

epidermal growth factor (EGF, 1.23 folds). TGC-CM contained more adiponectin (Figure 7B). In addition, TGO-CM contained higher levels of angiogenesis-related cytokines like matrix metallopeptidase 9 (MMP-9, 10.45 folds), serpin E1 (1.39 folds), and CX3CL-1 (2.02 folds), and contained fewer pro-inflammatory factors such as interleukin-1 α and β (IL-1 α and β, 0.67- and 0.47 folds, respectively), interleukin-6 (IL-6, 0.77 folds), macrophage colony-stimulating factor (M-CSF, 0.74 folds), and granulocyte colony-stimulating factor (G-CSF, 0.60 folds) (Figure 7C).
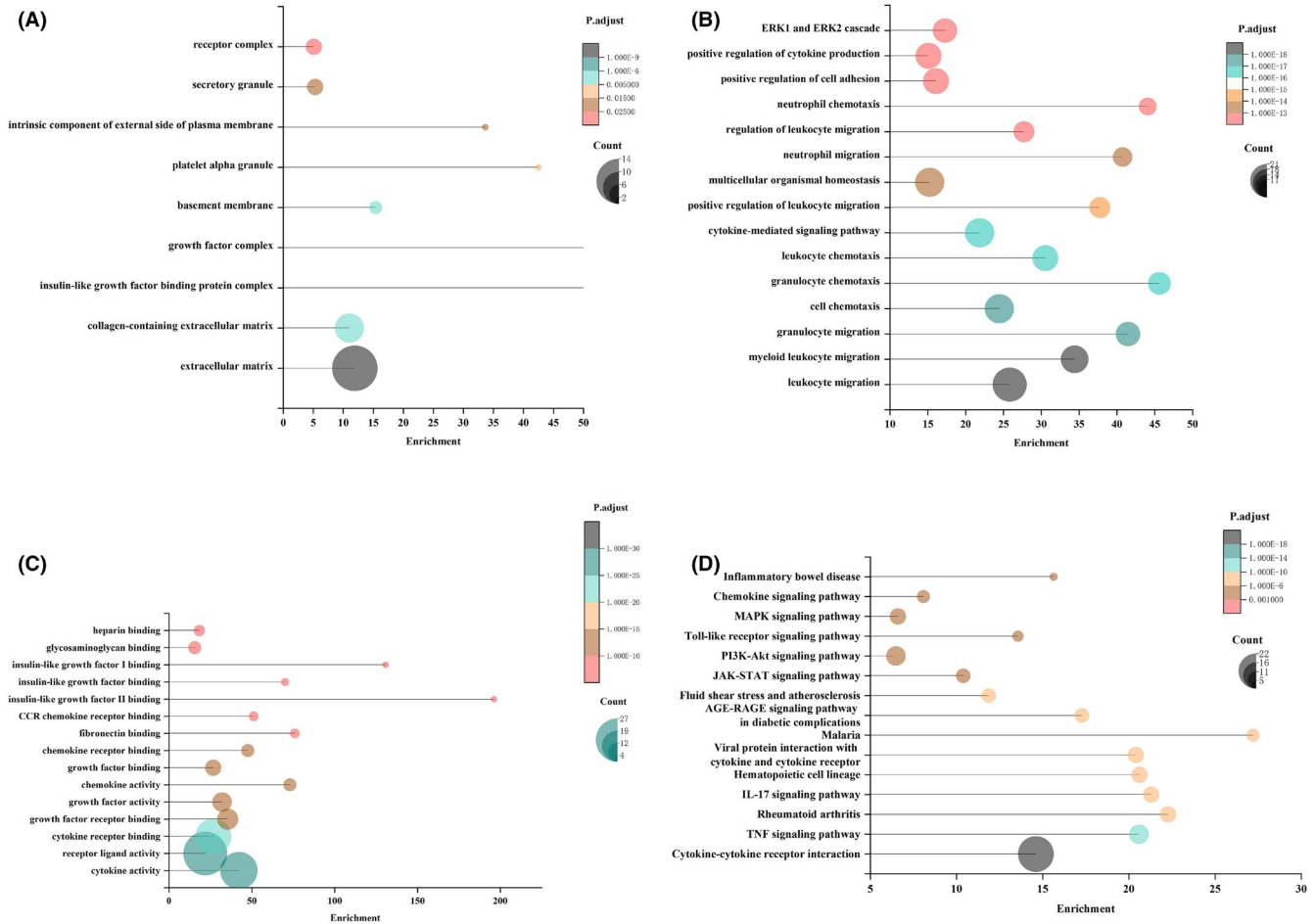
FIGURE 8 Possible mechanisms that led to the protein profile differences. (A) GO cellular component analysis: differential proteins mainly existed in forms of the receptor complex, secretory granule, growth factor complex, and extracellular matrix. (B) GO biological process analysis: differential proteins were mainly linked to cytokine production, positive cell adhesion regulation, and inflammatory processes. (C) GO molecular function analysis: differential proteins were functionally related to the activity and receptor bindings of growth factors, chemokines, and cytokines (D) KEGG analysis: cytokine–cytokine receptor interaction, TNF signalling pathway, and PI3K-Akt signalling pathway may be involved

3.7 | Possible mechanisms leading to the protein profile differences

GO cellular component analysis (Figure 8A) revealed that the differential proteins existed in forms of the receptor complex, secretory granule, growth factor complex, and extracellular matrix, with 5, 5, 6, and 23 detected protein types, respectively ($p < 0.05$). GO biological process analysis confirmed that these differential proteins were linked to cytokine production, positive cell adhesion regulation, and inflammatory processes (Figure 8B). These results aligned with the downregulated inflammation-related cytokine activity in TGO-CM (Figure 7C, $p < 0.05$). GO molecular function analysis (Figure 8C) revealed that these proteins were functionally related to the activity and receptor bindings of growth factors, chemokines, and cytokines ($p < 0.05$). KEGG analysis identified possible signalling mechanisms that led to such differential protein profile, including cytokine–cytokine receptor interaction, TNF signalling pathway, and PI3K-Akt signalling pathway (Figure 8D).

4 | DISCUSSION

Tooth germ comprises mesenchymal and epithelial components, and its organogenesis is a temporal interplay involving diverse biofactors between these two elements.[25,33] Successful CM production requires careful collection timing; 2D CM can be harvested between 24–72 h and every 2–4 days after seeding.[19] 3D ex vivo culture of tooth germs mimics the physiology of the original microenvironment, with hierarchical tissue structures and graded chemical distribution.[23,24] In our study of the 3D culture, hypoxia, undernutrition, and accumulation of metabolic waste resulted in greater damage at the organ core. The elevated apoptosis rate in tissue culture compared to that in cell line culture can distort the protein secretion profile[34]; excessive tissue debris and by-products may interfere with the subsequent CM content analysis.[35] Thus, to counter the tissue damage presented at 24 h and the low protein secretion at 8 h, 16 h was adopted as the harvest timing.

Vectors-mediated MSCs engineering has also been reported to successfully prime stem cells.[36,37] However, higher technique sensitivity, higher cost, and longer lab training curve have all limited its broad application from a clinical perspective. Besides, MSCs derived from parental pluripotent stem cells (PSC-MSCs) have shown advantages over adult MSCs such as higher homogeneity and proliferative potency.[38,39] Nevertheless, the human ethical concerns, cell availability, and subsequent cell expansion process all limited their application. Thus, in this study, we chose the TGC-CM and TGO-CM, instead of the direct engineered MSCs or PSC-MSCs, to prime DPSCs for pulp repair.

Compared with the 2D TGC-CM, the 3D TGO-CM demonstrated a superior DPSCs priming capability with improved cell proliferation, migration, in vitro mineralization, odontogenic differentiation, and angiogenesis. Conventional 2D CM-based revitalization therapy fails to regenerate truly functional dental pulp.[40] Odontoblast-like cells and vasculature are two intrinsic features of dentin–pulp complex regeneration. Non-collagenous proteins secreted by odontoblasts include odontogenesis-related DMP 1, DSP, BSP, and osteogenesis-related OSX.[41] VEGF plays a pivotal role in angiogenesis by promoting endothelial cell survival, proliferation, and migration.[42] Vasculature networks are essential in nutrient and cytokine delivery and metabolic waste transportation during pulp repair.[43]

Semi-orthotopic models using subcutaneous tooth fragment implantation have been broadly adopted to investigate pulp regeneration,[32,44–46] and such studies using 2D CM have demonstrated positive results of pulp–dentin complex regeneration. Here, we present the first semi-orthotopic model-based study to investigate DPSCs priming by 3D CM and DPSCs-mediated pulp repair. The formation of a well-organized pulp structure, robust vascular network, and odontogenic cell layer in the 3D TGO-CM group proved its superior regenerative capability over that of the 2D TGC-CM. However, no pre-dentin formation and odontoblast polarity were observed, which may be ascribed to the relatively short 4 weeks in vivo experimental time. Similar studies typically euthanize subjects after 12 weeks, providing sufficient time for hard tissue formation and odontoblast polarization.[32,44–46] We anticipate a proportionate trajectory in increased hard tissue formation and odontoblast polarization to accompany a longer timeline. Interestingly, the DMP1-positive cells were morphologically distinct, with flat and columnar structures in the 2D TGC-CM and 3D TGO-CM groups, respectively, indicating a polarization trend. The origin of the regenerated pulpal vasculature in this study remains unclear. Vasculature can be derived either from angiogenesis via host vessel growth, or from vasculogenesis via angiogenic DPSCs differentiation.[47] Here, lacking labelling analysis, we speculated that the neovascularization was angiogenesis which was derived from host vessel ingrowth through the end opening.[48] Summarily, in vitro and in vivo evidence confirmed the potential of 3D TGO-CM as a priming cocktail to enhance DPSCs-mediated pulp regeneration.

Proteome cytokine array, GOEA, and KEGG analysis revealed significant differences between the two CM secretome profiles. TGO-CM contains more growth factors such as FGF and EGF, which are related to cell proliferation and odontogenic differentiation.[2] Higher levels of angiogenesis-related factors such as angiopoietin-1, PDGF, VEGF, and FGF, in TGO-CM, contributed to vasculature formation.[49] Higher level of CX3CL-1, a type of chemokine with an angiogenic role,[50] was also detected in TGO-CM. In a clinical scenario, pulp blood perfusion is often limited by a narrow apical foramen or progressive inflammation,[51] potentially causing hypoxia in implanted DPSCs. 3D ex vivo culture of tooth germ mimics the in vivo graded oxygen distribution during germ development, with its inner core exhibiting increased hypoxia. As a self-protective response, the tooth germ elevates related gene expression, secreting more biofactors associated with cell survival, proliferation, and angiogenesis. Our results correspond with these observations, demonstrating that hypoxia can guide MSCs towards a pro-angiogenic phenotype and promote angiogenesis.[52–54]

Inflammation plays an important role in pulp regeneration,[55] as tissue repair can only occur at a lower inflammation resolution level.[56] An inflammatory biomolecules influx would impede regeneration due to cellular apoptosis and tissue necrosis[57,58]; however, low-intensity inflammation would stimulate positive pulp reparative responses.[59,60] Typical pro-inflammatory cytokines that govern the pulp inflammation process include interleukins like IL-1α/β and IL-6, collagenases like MMPs, colony-stimulating factors like M-CSF and G-CSF, and chemokines like CXCLs and CCLs.[61] MMP-3 promotes pulp regeneration in mild irreversible pulpitis by inhibiting IL-6 activity.[62] Wnt/β-catenin pathway activation in the noncanonical Wnt/Ca2+ pathway is implicated in impairing DPSC-based odontogenesis under inflammatory conditions.[63] Mild inflammatory conditions facilitate pulp repair through intracellular p38 MAPK and NF-κB signalling pathways.[59,60] Moreover, the paracrine function of MSCs could be strictly regulated by inflammatory signalling pathways like critical telomerase associated protein RAP 1/NF-kB signalling pathway.[64,65] Future efforts are still required to further elucidate the inflammation modulation and immunomodulation of MSCs. Here, in this study, the 3D TGO-CM created a mild inflammatory cocktail with less pro-inflammatory cytokines than the 2D TGC-CM.

The GO biological process analysis paralleled those of the molecular function analysis. Growth factors, cytokines, and chemokines are all present in TGO-CM. Though not entirely conclusive, the KEGG results imply that the differences between the secretome profiles may be attributable to the cytokine–cytokine receptor interaction and PI3K-Akt signalling pathway. Cytokines bind to receptors on the cell membrane surface, activate intracellular biomolecule interactions, and subsequently induce various cell behaviour, such as inflammatory responses. The PI3K-Akt signalling pathway plays a major role in cell apoptosis mitigation, proliferation, differentiation, and angiogenesis.[66] Growth factors bind to protein G-linked receptors, activate P13K/AKT, and induce subsequent cell activities. Hypoxia promotes angiogenesis via the interaction between hypoxia-inducible factor-1α (HIF-1α) and the P13K/AKT signalling pathway.[67] In this study, the biomimic-graded hypoxia inside 3D cultured tooth germs may induce the production of pro-angiogenic biomolecules as an adaptive response.

Due to budget and time constraints, we were unable to address certain limitations. Future efforts may focus on the following aspects: influence of factors such as different embryonic stages of tooth germs, priming duration, and pathological status on protein profiles; more thorough filtering of effective CM components; in-depth mechanisms leading to different secretome profiles; use of orthotopic models of larger animals and longer-term follow-up; optimizing and standardizing the fabrication protocols of 3D CM before use.

5 | CONCLUSION

Dental pulp stem cells-based pulp regeneration exhibit shortcomings, and its therapeutic outcomes rely heavily on the unreliable post-implantation functional status of stem cells. In this study, we prepared CM of 3D tooth germ organ and investigated its pre-conditioning capabilities on DPSCs for early dental pulp regeneration on a semi-orthotopic tooth fragment model in nude mice. 3D TGO-CM primed DPSCs exhibited higher cell proliferation, migration, in vitro mineralization, odontogenic differentiation, and angiogenesis. Moreover, 3D TGO-CM priming achieved superior early in vivo pulp regeneration results, with well-organized pulp structures, odontogenic cell layer attachment, and increased vasculature formation at 4 weeks post-surgery. 3D TGO-CM contained more growth factors related to odontogenesis and angiogenesis and fewer pro-inflammatory cytokines. Cytokine–cytokine receptor interaction and PI3K-Akt signalling pathway may account for the differential protein profiles of the two CM types.

To the best of our knowledge, this is the first study to investigate the protein profile of 3D tooth germs and the first to apply it for early in vivo pulp regeneration. Taken together, our results confirmed that 3D TGO-CM can be applied as a priming cocktail to enhance DPSCs-mediated early pulp regeneration. This study may shed light on personalized stem cell priming for early pulp regeneration using a trace-back-to-organ approach.

CONFLICT OF INTEREST
There are no conflicts of interest in this study.

DATA AVAILABILITY STATEMENT
Data are available from the corresponding author upon reasonable request.

ORCID
Tengfei Zhou https://orcid.org/0000-0001-9370-2527
Zhihui Tian https://orcid.org/0000-0002-6423-2113

REFERENCES
1. Yoshida S, Tomokiyo A, Hasegawa D, Hamano S, Sugii H, Maeda H. Insight into the role of dental pulp stem cells in regenerative therapy. *Biology*. 2020;9(7):160.
2. Tsutsui TW. Dental pulp stem cells: advances to applications. *Stem Cells Cloning: Adv Appl*. 2020;13:33-42.
3. Yamada Y, Nakamura-Yamada S, Konoki R, Baba S. Promising advances in clinical trials of dental tissue-derived cell-based regenerative medicine. *Stem Cell Res Ther*. 2020;11(1):175.
4. Sugimura-Wakayama Y, Katagiri W, Osugi M, et al. Peripheral nerve regeneration by secretomes of stem cells from human exfoliated deciduous teeth. *Stem Cells Dev*. 2015;24(22):2687-2699.
5. Nuñez J, Vignoletti F, Caffesse RG, Sanz M. Cellular therapy in periodontal regeneration. *Periodontol 2000*. 2019;79(1):107-116.
6. Zhang LX, Shen LL, Ge SH, et al. Systemic BMSC homing in the regeneration of pulp-like tissue and the enhancing effect of stromal cell-derived factor-1 on BMSC homing. *Int J Clin Exp Pathol*. 2015;8(9):10261-10271.
7. Zong Z, Zhang X, Yang Z, et al. Rejuvenated ageing mesenchymal stem cells by stepwise preconditioning ameliorates surgery-induced osteoarthritis in rabbits. *Bone Joint Res*. 2021;10(1):10-21.
8. Lukomska B, Stanaszek L, Zuba-Surma E, Legosz P, Sarzynska S, Drela K. Challenges and controversies in human mesenchymal stem cell therapy. *Stem Cells Int*. 2019;2019(2):1-10.
9. Squillaro T, Peluso G, Galderisi U. Clinical trials with mesenchymal stem cells: an update. *Cell Transplant*. 2016;25(5):829-848.
10. Tyndall A. Successes and failures of stem cell transplantation in autoimmune diseases. *Hematology Am Soc Hematol Educ Program*. 2011;2011(1):280-284.
11. Ferreira JR, Teixeira GQ, Santos SG, Barbosa MA, Almeida-Porada G, Gonçalves RM. Mesenchymal stromal cell secretome: influencing therapeutic potential by cellular pre-conditioning. *Front Immunol*. 2018;9:2837.
12. Park H, Park H, Mun D, et al. Extracellular vesicles derived from hypoxic human mesenchymal stem cells attenuate GSK3β expression via miRNA-26a in an ischemia-reperfusion injury model. *Yonsei Med J*. 2018;59(6):736-745.
13. Novais A, Lesieur J, Sadoine J, et al. Priming dental pulp stem cells from human exfoliated deciduous teeth with fibroblast growth factor-2 enhances mineralization within tissue-engineered constructs implanted in craniofacial bone defects. *Stem Cells Transl Med*. 2019;8(8):844-857.
14. Kang H, Kim KH, Lim J, et al. The therapeutic effects of human mesenchymal stem cells primed with sphingosine-1 phosphate on pulmonary artery hypertension. *Stem Cells Dev*. 2015;24(14):1658-1671.
15. Petrenko Y, Syková E, Kubinová Š. The therapeutic potential of three-dimensional multipotent mesenchymal stromal cell spheroids. *Stem Cell Res Ther*. 2017;8(1):94.
16. Sandonà M, Di Pietro L, Esposito F, et al. Mesenchymal stromal cells and their secretome: new therapeutic perspectives for skeletal muscle regeneration. *Front Bioeng Biotech*. 2021;9:652970.
17. Bogatcheva NV, Coleman ME. Conditioned medium of mesenchymal stromal cells: a new class of therapeutics. *Biochemistry(Mosc)*. 2019;84(11):1375-1389.

18. Miceli V, Bulati M, Iannolo G, Zito G, Gallo A, Conaldi PG. Therapeutic properties of mesenchymal stromal/stem cells: the need of cell priming for cell-free therapies in regenerative medicine. *Int J Mol Sci*. 2021;22(2):763.

19. Kichenbrand C, Velot E, Menu P, Moby V. Dental pulp stem cell-derived conditioned medium: an attractive alternative for regenerative therapy. *Tissue Eng Part B*. 2019;25(1):78-88.

20. Wang YX, Ma ZF, Huo N, et al. Porcine tooth germ cell conditioned medium can induce odontogenic differentiation of human dental pulp stem cells. *J Tissue Eng Regener Med*. 2011;5(5):354-362.

21. Li TX, Yuan J, Chen Y, et al. Differentiation of mesenchymal stem cells from human umbilical cord tissue into odontoblast-like cells using the conditioned medium of tooth germ cells in vitro. *BioMed Res Int*. 2013;2013(7):218543.

22. Chen Y, Liu H. The differentiation potential of gingival mesenchymal stem cells induced by apical tooth germ cell-conditioned medium. *Mol Med Rep*. 2016;14(4):3565-3572.

23. Chaicharoenaudomrung N, Kunhorm P, Noisa P. Three-dimensional cell culture systems as an in vitro platform for cancer and stem cell modeling. *World J Stem Cells*. 2019;11(12):1065-1083.

24. Bingel C, Koeneke E, Ridinger J, et al. Three-dimensional tumor cell growth stimulates autophagic flux and recapitulates chemotherapy resistance. *Cell Death Dis*. 2017;8(8):e3013.

25. Balic A. Biology explaining tooth repair and regeneration: a mini-review. *Gerontology*. 2018;64(4):382-388.

26. Kumar A, Kumar V, Rattan V, Jha V, Pal A, Bhattacharyya S. Molecular spectrum of secretome regulates the relative hepatogenic potential of mesenchymal stem cells from bone marrow and dental tissue. *Sci Rep*. 2017;7(1):15015.

27. Tachida Y, Sakurai H, Okutsu J, et al. Proteomic comparison of the secreted factors of mesenchymal stem cells from bone marrow, adipose tissue and dental pulp. *J Protemoics Bioinf*. 2015;8:12.

28. He L, Zhou J, Chen M, et al. Parenchymal and stromal tissue regeneration of tooth organ by pivotal signals reinstated in decellularized matrix. *Nat mat*. 2019;18(6):627-637.

29. Liu Y, Sun Y, Li S, et al. Tetrahedral framework nucleic acids based delivery of antimicrobial peptides with improved effects and alleviated susceptibility to bacterial degradation. *Nano Lett*. 2020;20(5):3602-3610.

30. Chen J, Xu H, Xia K, Cheng S, Zhang Q. Resolvin E1 accelerates pulp repair by regulating inflammation and stimulating dentin regeneration in dental pulp stem cells. *Stem Cell Res Ther*. 2021;12(1):75.

31. Cui D, Xiao J, Zhou Y, et al. Epiregulin enhances odontoblastic differentiation of dental pulp stem cells via activating MAPK signaling pathway. *Cell Prolif*. 2019;52(6):e12680.

32. Zhuang X, Ji L, Jiang H, et al. Exosomes derived from stem cells from the apical papilla promote dentine-pulp complex regeneration by inducing specific dentinogenesis. *Stem Cells Int*. 2020;2020(4):1-10.

33. Tian Z, Lv X, Zhang M, et al. Deletion of epithelial cell-specific Cdc42 leads to enamel hypermaturation in a conditional knockout mouse model. *Biochim Biophys Acta Mol Basis Dis*. 2018;1864(8):2623-2632.

34. Yao L, Lao W, Zhang Y, et al. Identification of EFEMP2 as a serum biomarker for the early detection of colorectal cancer with lectin affinity capture assisted secretome analysis of cultured fresh tissues. *J Proteome Res*. 2012;11(6):3281-3294.

35. Sarkar P, Randall SM, Muddiman DC, Rao BM. Targeted proteomics of the secretory pathway reveals the secretome of mouse embryonic fibroblasts and human embryonic stem cells. *Mol Cell Proteomics*. 2012;11(12):1829-1839.

36. Gnecchi M, He H, Liang OD, et al. Paracrine action accounts for marked protection of ischemic heart by Akt-modified mesenchymal stem cells. *Nat Med*. 2005;11(4):367-368.

37. Liang X, Ding Y, Lin F, et al. Overexpression of ERBB4 rejuvenates aged mesenchymal stem cells and enhances angiogenesis via PI3K/AKT and MAPK/ERK pathways. *FASEB J*. 2019;33(3):4559-4570.

38. Zhang J, Chan YC, Ho JC, Siu CW, Lian Q, Tse HF. Regulation of cell proliferation of human induced pluripotent stem cell-derived mesenchymal stem cells via ether-à-go-go 1 (hEAG1) potassium channel. *Am J Physiol Cell Physiol*. 2012;303(2):C115-C125.

39. Sze SK, de Kleijn DP, Lai RC, et al. Elucidating the secretion proteome of human embryonic stem cell-derived mesenchymal stem cells. *Mol Cell Proteomics*. 2007;6(10):1680-1689.

40. Morotomi T, Washio A, Kitamura C. Current and future options for dental pulp therapy. *Jan Dent Sci Rev*. 2019;55(1):5-11.

41. Ching HS, Luddin N, Rahman IA, Ponnuraj KT. Expression of odontogenic and osteogenic markers in DPSCs and SHED: a review. *Curr Stem Cell Res Therapy*. 2017;12(1):71-79.

42. Breier G. Functions of the VEGF/VEGF receptor system in the vascular system. *Semin Thromb Hemostasis*. 2000;26(5):553-559.

43. Rombouts C, Giraud T, Jeanneau C, About I. Pulp vascularization during tooth development, regeneration, and therapy. *J Dent Res*. 2017;96(2):137-144.

44. Chen YJ, Zhao YH, Zhao YJ, et al. Potential dental pulp revascularization and odonto-/osteogenic capacity of a novel transplant combined with dental pulp stem cells and platelet-rich fibrin. *Cell Tissue Res*. 2015;361(2):439-455.

45. Huang GT, Yamaza T, Shea LD, et al. Stem/progenitor cell-mediated de novo regeneration of dental pulp with newly deposited continuous layer of dentin in an in vivo model. *Tissue Eng, Part A*. 2010;16(2):605-615.

46. Zhu X, Liu J, Yu Z, et al. A miniature swine model for stem cell-based de novo regeneration of dental pulp and dentin-like tissue. *Tissue Eng, Part C*. 2018;24(2):108-120.

47. Shi W, Xin Q, Yuan R, Yuan Y, Cong W, Chen K. Neovascularization: the main mechanism of MSCs in ischemic heart disease therapy. *Front Cardiovasc Med*. 2021;8:633300.

48. Nakashima M, Iohara K, Bottino MC, Fouad AF, Nör JE, Huang GT. Animal models for stem cell-based pulp regeneration: foundation for human clinical applications. *Tissue Eng, Part B*. 2019;25(2):100-113.

49. Maacha S, Sidahmed H, Jacob S, et al. Paracrine mechanisms of mesenchymal stromal cells in angiogenesis. *Stem Cells Int*. 2020;2020:1-12.

50. Park Y, Lee J, Kwak JY, et al. Fractalkine induces angiogenic potential in CX3CR1-expressing monocytes. *J leukocyte biol*. 2018;103(1):53-66.

51. Schmalz G, Widbiller M, Galler KM. Clinical perspectives of pulp regeneration. *J Endodont*. 2020;46(9s):s161-s174.

52. Lee SG, Joe YA. Autophagy mediates enhancement of proangiogenic activity by hypoxia in mesenchymal stromal/stem cells. *Biochem Biophys Res Commun*. 2018;501(4):941-947.

53. Isik B, Thaler R, Goksu BB, et al. Hypoxic preconditioning induces epigenetic changes and modifies swine mesenchymal stem cell angiogenesis and senescence in experimental atherosclerotic renal artery stenosis. *Stem Cell Res Ther*. 2021;12(1):240.

54. Gao W, He R, Ren J, et al. Exosomal HMGB1 derived from hypoxia-conditioned bone marrow mesenchymal stem cells increases angiogenesis via the JNK/HIF-1α pathway. *FEBS Open Bio*. 2021;11(5):1364-1373.

55. Fawzy El-Sayed KM, Elsalawy R, Ibrahim N, et al. The dental pulp stem/progenitor cells-mediated inflammatory-regenerative axis. *Tissue Eng, Part B*. 2019;25(5):445-460.

56. Zhang M, Zhang X, Tian T, et al. Anti-inflammatory activity of curcumin-loaded tetrahedral framework nucleic acids on acute gouty arthritis. *Bioact Mater*. 2021;8:368-380. doi:10.1016/j.bioactmat.2021.06.003

57. Lara VS, Figueiredo F, da Silva TA, Cunha FQ. Dentin-induced in vivo inflammatory response and in vitro activation of murine macrophages. *J Dent Res*. 2003;82(6):460-465.

58. Liu Y, Wang L, Kikuiri T, et al. Mesenchymal stem cell-based tissue regeneration is governed by recipient T lymphocytes via IFN-γ and TNF-α. *Nat Med*. 2011;17(12):1594-1601.

59. He W, Wang Z, Luo Z, et al. LPS promote the odontoblastic differentiation of human dental pulp stem cells via MAPK signaling pathway. *J Cell Physiol*. 2015;230(3):554-561.

60. Feng X, Feng G, Xing J, et al. TNF-α triggers osteogenic differentiation of human dental pulp stem cells via the NF-κB signaling pathway. *Cell Biol Int*. 2013;37(12):1267-1275.

61. Cooper PR, Chicca IJ, Holder MJ, Milward MR. Inflammation and regeneration in the dentin–pulp complex: net gain or net loss? *J Endodont*. 2017;43(9s):s87-s94.

62. Eba H, Murasawa Y, Iohara K, et al. The anti-inflammatory effects of matrix metalloproteinase-3 on irreversible pulpitis of mature erupted teeth. *PLoS One*. 2012;7(12):e52523.

63. Liu N, Shi S, Deng M. High levels of β-catenin signaling reduce osteogenic differentiation of stem cells in inflammatory microenvironments through inhibition of the noncanonical Wnt pathway. *J Bone Miner Res*. 2011;26(9):2082-2095.

64. Ding Y, Liang X, Zhang Y, et al. Rap1 deficiency-provoked paracrine dysfunction impairs immunosuppressive potency of mesenchymal stem cells in allograft rejection of heart transplantation. *Cell Death Dis*. 2018;9(3):386.

65. Zhang Y, Chiu S, Liang X, et al. Rap1-mediated nuclear factor-kappaB (NF-κB) activity regulates the paracrine capacity of mesenchymal stem cells in heart repair following infarction. *Cell Death Discov*. 2015;1:15007.

66. Liu F, Huang X, Luo Z, et al. Hypoxia-activated PI3K/Akt inhibits oxidative stress via the regulation of reactive oxygen species in human dental pulp cells. *Oxid Med Cell Longevity*. 2019;2019:6595189.

67. Song W, Liang Q, Cai M, Tian Z. HIF-1α-induced up-regulation of microRNA-126 contributes to the effectiveness of exercise training on myocardial angiogenesis in myocardial infarction rats. *J cell mol med*. 2020;24(22):12970-12979.

SUPPORTING INFORMATION

Additional supporting information may be found in the online version of the article at the publisher's website.